α-Chitin Nanocrystals Prepared from Shrimp Shells and Their Specific Surface Area Measurement

Jacob D. Goodrich and William T. Winter*

Cellulose Research Institute and Department of Chemistry, SUNY College of Environmental Science and Forestry, Syracuse, New York 13210

Received April 13, 2006; Revised Manuscript Received September 15, 2006

α-Chitin was isolated from shrimp shells. The chitin was subjected to extensive treatments of acid hydrolysis and mechanical disruption to yield nanocrystals. The goal of this article is to characterize α-chitin nanocrystals produced from shrimp shells in regard to crystallite properties and the specific surface area of the chitin nanoparticles. X-ray diffraction data indicate an increase in chitin crystallinity after hydrolysis, as less-ordered chitin domains are digested. Line broadening data were used to measure crystallite size and particle size in the hydrolyzed chitin nanocrystals. Dye adsorption with Congo red was used to measure the specific surface area of the particles, indicating values near 350 m^2/g. This value was supported with calculations derived from X-ray crystallite size measurements. Particle surface area measurements were compared with similarly prepared cellulose nanocrystals.

Introduction

Chitin is a major component in the supporting tissues of organisms such as crustaceans, fungi, and insects.[1] Next to cellulose, it is the most abundant biopolymer found in nature. Chitin is structurally similar to cellulose and is a linear polysaccharide containing β-(1→4)-2-deoxy-2-acetamido-D-glucopyranose repeating units. Supporting tissues containing chitin generally exist as naturally occurring composites. In the exoskeletons of crustaceans, chitin is intimately associated with other materials such as proteins, lipids, calcium carbonate, and pigments. The chitin molecules are known to order into helicoidal, microfibrillar structures that are embedded into the protein material of the shells.[2] The lateral dimensions of the microfibrils can range from 2.5 to 25 nm, depending upon the source organism.[2] From shrimp shells, chitin can be isolated from the cuticle by a series of decalcification and deproteinization steps using acid and alkali treatments, respectively.[3,4] Subjecting the isolated chitin to repetitive acid hydrolysis treatments randomly cleaves the noncrystalline regions of the microfibrils to produce stable colloidal suspensions of rodlike particles of nanometer dimensions.[2,5] Such chitin nanoparticles have been prepared from various sources such as lobster tendons,[6] crab shells,[5,7] and squid pens[8] and studied primarily for their applications in fiber-reinforced nanocomposites. The appeal of chitin nanoparticles as fiber reinforcements lies in their advantageous properties, such as small size and high particle aspect ratio, high surface area, high stiffness and strength, wide availability and renewability, low density, and ease of chemical modification.[7,9,10] Several reports have been published regarding the use of chitin nanoparticles as fiber reinforcements in both natural and synthetic polymer matrixes.[7−11]

An important aspect that influences the successful performance of a composite is the interaction of the particle reinforcement phase with the surrounding matrix. Possible routes to improving interfacial interactions involve increasing the particle surface area and introducing compatibilizing agents through surface functionalization or other means. The high aspect ratio observed for rigid carbohydrate nanoparticles such as cellulose and chitin is often mentioned, but little information has been published regarding their surface areas.

The aim of this article is to characterize and measure the specific surface area (SSA) of α-chitin nanocrystals produced from shrimp shells. With this knowledge, it is hoped that the understanding of particle interactions in chitin-based nanocomposites will be improved. Characterization methods include surface area measurements by uptake of Congo red dye, crystallite dimensions by line broadening methods, degree of crystallinity by X-ray diffraction, transmission and scanning electron microscopy, ^{13}C cross-polarization magic-angle spinning (CP-MAS) NMR, and Fourier transform infrared spectroscopy.

In this study, we have prepared and characterized α-chitin nanocrystals from shrimp shells. A dye adsorption technique was used for measuring the specific surface areas of the chitin before and after nanoparticle preparation. The dye, Congo red, has been used to assess specific surface areas of cellulose substrates such as cotton fibers, microfibrillated cellulose, and wood pulp.[12,13] More conventional methods of specific surface area measurements for nanoparticles include nitrogen sorption and mercury porosimetry; however, these methods are only applicable to dry materials. The drying process often induces agglomeration in chitin and cellulose, and therefore such techniques applied to dry chitin or cellulose significantly underestimate the specific surface area.[14] Dye binding experiments are able to measure specific surface areas of cellulose and chitin as swollen dispersed materials. These measurements are more practical when considering the application of chitin nanocrystals in thermoplastic composites, where the particles are well dispersed and in some cases swollen. In addition, specific surface area estimates calculated from line broadening information in X-ray powder diffraction experiments were found to be in reasonable agreement with measurements from the dye adsorption method.

Materials and Methods

Raw Materials. The chitin used in this work was extracted from shrimp purchased at a local food retailer. Sodium hydroxide pellets

* Corresponding author. Telephone: (315) 470-6876. Fax: (315) 470-6856. E-mail: wtwinter@syr.edu.

10.1021/bm0603589 CCC: $37.00
Published on Web 11/29/2006

were of reagent grade purchased from Mallinckrodt (St. Louis, MO). Hydrochloric acid (37% w/w) was purchased from EM Science (Cherry Hill, NJ) and further diluted. The acetone, methanol, and ethanol used were reagent grade purchased from Pharmco (Brookfield, CT). Congo red was purchased from Aldrich (Milwaukee, WI) and subjected to further purification by Soxhlet extraction twice with 87.5% 2-propanol/12.5% distilled water for 6 h.[14]

Isolation of Chitin from Shrimp Shells. After the shrimp were deshelled, the shells were soaked in 0.5 M NaOH at room temperature for 24 h to remove loosely associated proteins and lipids.[3] The shells were rinsed with distilled water until a neutral pH was reached and subsequently dried in a vacuum oven at 50 °C for 48 h. The dry shells were milled to 40-mesh particle size with a bench top Wiley mill. The granulated shrimp shells were demineralized by a treatment with 0.25 M HCl for 45 min at room temperature.[4] The material was filtered in a Büchner funnel on Whatman No. 1 filter paper and rinsed to neutrality with distilled water. All subsequent filtrations were performed under the same conditions. Protein was removed from the material by three repeated six-hour treatments with 2.5 M NaOH at 80 °C.[3] Filtration and rinsing were done between successive repetitions of the deproteinization step. The resulting chitin material was still slightly pink in color. The chitin was rinsed three times each in acetone and ethanol to remove organic soluble compounds and dried in a vacuum oven at 40 °C for several days.[3] The final product was a white fluffy powder.

Preparation of Shrimp Shell Chitin Nanocrystals. The purified chitin was hydrolyzed in 3 M HCl for 1.5 h at 90 °C to digest the disordered regions, thereby decreasing particle size. This process was repeated three times with the chitin recovered by centrifugation after each hydrolysis. Following the final hydrolysis step, the chitin was recovered by centrifugation and resuspended in distilled water to reduce the acid concentration. This chitin suspension was then dialyzed against several changes of distilled water until a pH of 6 was reached. Dialysis was performed with SpectraPor 10K to 12K MWCO regenerated cellulose dialysis membranes from Spectrum Laboratories. The final neutralized chitin nanocrystal suspension was then blended in a Cuisinart blender at high speed for 5 min. The resulting fine suspension was further dispersed in water by homogenization at 8000 psi for 10−15 cycles with an APV Gaulin 1000 homogenizer. Dry chitin nanocrystals were prepared by lyophilizing the homogenized aqueous suspension.

Microscopy. Transmission electron microscopy imaging was performed on a JEOL JEM-2000EX transmission microscope operated at an acceleration voltage of 80 kV. One drop of the chitin nanocrystal suspension (0.01 wt % in distilled water) was deposited on a Formvar/carbon-coated copper grid and allowed to air-dry.

Scanning electron microscopy analysis was performed on a JEOL JSM-5800LV microscope operating at an accelerating voltage of 20 kV. The chitin samples were adhered to the sample stubs with conductive carbon tape and sputter-coated with Au/Pd prior to analysis.

Spectroscopic Analysis. Attenuated total reflectance-Fourier transform infrared spectroscopy (ATR-FTIR) was used to analyze the surface of the chitin nanoparticles. The ATR-FTIR spectrum of dry powdered chitin nanoparticles was acquired with a Bio-Rad FTS6000 spectrometer. The configuration used a Harrick SplitPea accessory, a silicon ATR crystal, and a deuterated triglycine sulfate pyroelectric detector. The sampling area was 250 μm × 250 μm with a spectral resolution of 4 cm^{-1}.

Solid samples were packed in 7-mm zirconium ceramic rotors, and solid-state CP-MAS ^{13}C NMR spectra were obtained at 75 MHz using a 300 MHz Bruker Avance spectrometer. The spinning rate was 7.0 kHz with 1-ms contact times and 5-s delay between scans.[15] The sample was acquired using a cptppm2 pulse program. The spectrum shown is an average of 2048 scans with 1246 data points.

X-ray Analysis. The X-ray powder diffraction analysis was done using a rotating anode X-ray source (Rigaku DMAX-1000) operated at 50 kV and 120 mA and generating Ni-filtered Cu Kα radiation (λ = 0.15419 nm). Typical diffraction patterns were collected as the sum of five individual scans from 5° to 50° in 2θ at 10°/min and an increment of 0.048°; thus, 940 data points were collected per scan. Curve deconvolution of the X-ray data was accomplished using the Peak Fit v.4 software package from AISN Software Co.

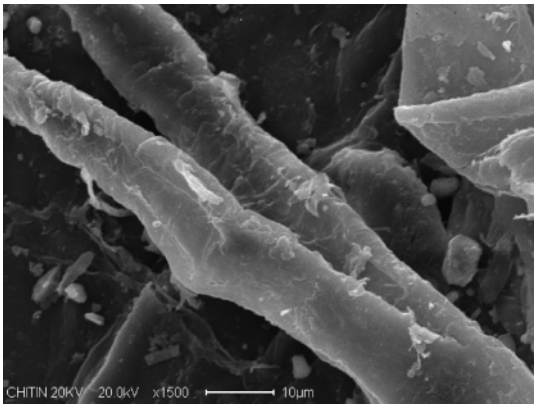

Figure 1. SEM micrograph of chitin fibers isolated from shrimp shells. Actual magnification shown is ×1200.

Surface Area Study. Specific surface area measurements were performed by Congo red dye adsorption experiments as described by Inglesby and Zeronian.[12] A chitin nanocrystal suspension was dialyzed (10K−12K MWCO tubing) against a 0.1 M phosphate buffer (pH = 6) for several days with multiple changes of the buffer solution. A 0.0266% (w/v) chitin nanocrystal suspension in the buffer was dyed with various concentrations of Congo red dye (5−30% of the weight of substrate) at 60 °C for 24 h. A small amount of NaCl (0.004 wt %) was added to each sample at the start of the experiment to neutralize charged surface sites on the chitin and cellulose nanocrystals. After 24 h, the samples were centrifuged for 10 min, the supernatant was drawn off, and its absorbance was measured at 488 nm with a Beckman DU-600 spectrophotometer. Other chitin and cellulose substrates in this experiment were subjected to the same experimental procedure as that described above. All runs were at the least duplicated, with the reported values being the averages. The maximal adsorption of Congo red dye on the chitin substrates was calculated using an equation derived from monolayer adsorption theory.

The bacterial cellulose and pulp cellulose used in the surface area study were provided by CPKelco (San Diego, CA) and Weyerhaeuser (Cosmopolis, WA), respectively. Cellulose nanocrystals were prepared from the pure material using a previously described hydrolysis procedure with 65 wt % sulfuric acid for 1.5 h.[16] The length and number of hydrolysis and homogenization treatments were the same for those used to prepare the chitin nanocrystals.

HCl treatment on chitin and H_2SO_4 treatment on cellulose both yield surface-charged materials, allowing for a better comparison between the two species in the dye adsorption study.[2,16]

Results and Discussion

Microscopy. After purification, acid hydrolysis, and mechanical disruption, SEM and TEM techniques were used to observe the products. Figure 1 shows an SEM micrograph of purified shrimp shell chitin prior to hydrolysis and homogenization. The particle dimensions for the isolated fibers are observed to be between 5 and 10 μm in width and several hundred micrometers in length. Figure 2 is a TEM micrograph of chitin nanocrystals cast from a dilute suspension. The lateral dimensions of the chitin nanoparticles range from 200 to 500 nm, while the transverse dimensions are about 10 to 15 nm for individual nanocrystals.

ATR-FTIR Analysis. FTIR analysis was used to assess the purity of the chitin nanoparticles and to observe the presence of any residual surface bound proteins. Figure 3 indicates that

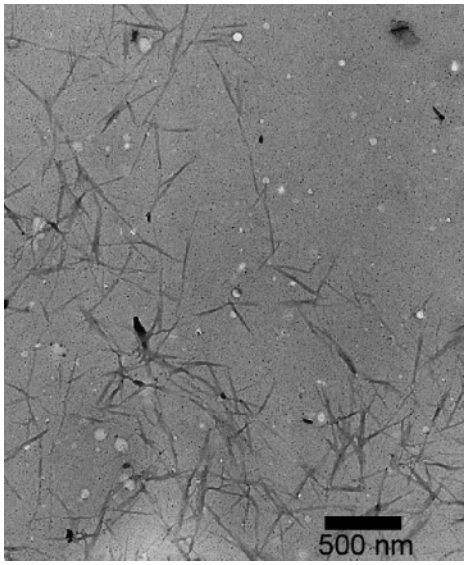

Figure 2. TEM micrograph of chitin nanocrystals from shrimp shells formed after hydrolysis and mechanical dispersion. Magnification shown is ×10 000.

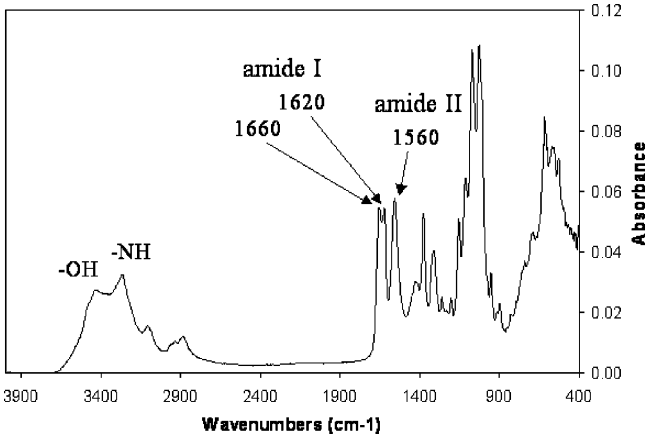

Figure 3. ATR-FTIR spectrum of chitin nanoparticles. Spectral features indicate pure α-chitin.

the material is pure α-chitin with split absorbance peaks at 1660 and 1620 cm^{-1} corresponding to the amide I region and an absorbance peak at 1560 cm^{-1} corresponding to the amide II region. The spectrum is lacking a signal at 1540 cm^{-1}, where proteins would normally give rise to absorption.[17] From this it is evident that the chitin is pure of any protein material.

NMR Analysis. ^{13}C CP-MAS NMR spectroscopy was used to estimate an average degree of N-acetylation (DA) for the chitin nanocrystals and to assess changes in acetylation after hydrolysis. Using a 5-s relaxation delay and a contact time of 1 ms for the acquisition of the ^{13}C CP-MAS NMR spectra, we can achieve near quantitative results.[18] The DA was determined by the ratio of the integration values of the methyl carbon to the anomeric carbon signal. The methyl signal was chosen over the carbonyl signal because of the attached protons, which allow for better magnetization transfer in the cross-polarization experiment.

The DA from CP-MAS NMR was calculated to be 0.90 for the chitin nanocrystals after hydrolysis and 0.89 prior to hydrolysis, indicating that the hydrolysis treatment had little effect on the DA. Figure 4 shows the NMR spectra for shrimp shell chitin nanocrystals.

Signal assignments are shown in Figure 4 and were based upon an article published by Tanner et al.[19] From the spectrum in Figure 4, it is also evident that the isolated chitin nanocrystals are pure and residual proteins and minerals are absent. The spectrum for the pure chitin sample is not noticeably different from the nanocrystal data and is not shown.

X-ray Analysis. X-ray powder diffraction was performed to monitor the changes in crystallinity and morphology of the chitin nanocrystals after hydrolysis and to estimate crystallite sizes in the chitin samples. Figure 5 shows the diffraction patterns of the chitin nanocrystals and the pure shrimp shell chitin prior to hydrolysis. The diffraction patterns for both materials show typical reflections of pure α-chitin, indicating that the crystal integrity is maintained after hydrolysis.

Through curve deconvolution of the data from native chitin and the hydrolyzed chitin nanocrystals, an increase in the crystallinity was observed after hydrolysis. To determine sample crystallinity, the diffraction data was smoothed by a Savitzky−Golay filter using a second-order polynomial regression with 10 points and deconvoluted and fit with Gaussian−Lorentzian line shapes in the Peak Fit v.4 software package. This method of peak fitting provided a reasonable overall curve fit with a correlation coefficient of 0.95 for all samples The six most intense crystalline diffraction peaks were observed for $5° \leq 2\theta \leq 30°$ and were indexed as the 020, 021, 110, 120, 130, and 013 reflections according to the structure of α-chitin.[20] The curve deconvolution for the chitin nanocrystals is shown in Figure 6 as an example.

Deconvolution assumed the 2θ values predicted by the reported structure of α-chitin as seen in Table 1.

The crystallinity was measured as the ratio of the sum of the areas under the crystalline diffraction peaks to the total area under the curve for $5° \leq 2\theta \leq 30°$, on the basis of a method proposed for cellulose and used here for chitin.[21] From this analysis, we found the percent crystallinity of the pure shrimp shell chitin to be approximately 76% and increasing to 84% for the nanocrystals after acid hydrolysis and homogenization. This signifies a reduction in the amorphous contribution to the diffraction data and suggests that some of the amorphous regions in the cellulose are digested during the hydrolysis process. The intensity of the chitin nanocrystal diffraction peaks is slightly less than that of the pure chitin, indicating that some crystalline domains were mildly affected by the hydrolysis treatment. However, with the increasing percent crystallinity upon hydrolysis, the losses due to the digestion of the amorphous material are greater than the losses to the crystalline material.

Information regarding the average crystallite sizes for the chitin materials was also extracted from the deconvoluted X-ray diffraction data. Curve deconvolution assisted in measuring the peak widths at half-maximum intensity so that crystallite size could be calculated using the Scherrer relation:

$$D_{hkl} = (0.9)(\lambda_{CuK\alpha})/(\text{fwhm})_{hkl}(\cos\theta)_{hkl}$$

where fwhm is the full width at half-maximum in radians for the particular Bragg peak. The fwhm is used to measure the line broadening, which is assumed to arise from the finite size of the crystallites. Disordered domains reflecting at Bragg angles and instrumental factors can contribute to line broadening as well and tend to be a source of error. On the basis of crystallographic studies of α-chitin from various sources, it is apparent that the molecular repeat axis and the microfibrillar axis are coincident, so that the 001 set of planes corresponds to the longitudinal axis of the microfibrils.[20,22−24] It has also been previously shown that the 100 set of planes corresponds to the growth plane for α-chitin.[22] Given the orthorhombic geometry of the crystals, if the 001 set of planes represents the longitudinal

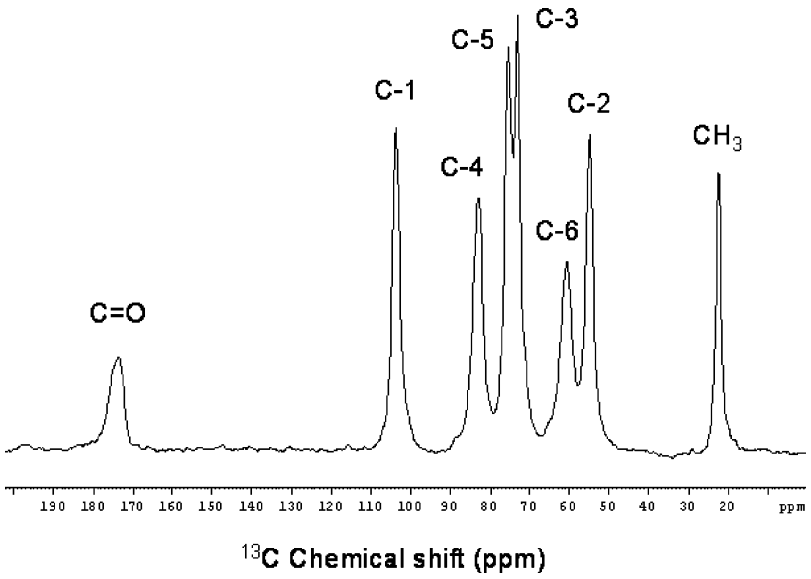

Figure 4. ^{13}C CP-MAS spectrum of chitin nanocrystals.

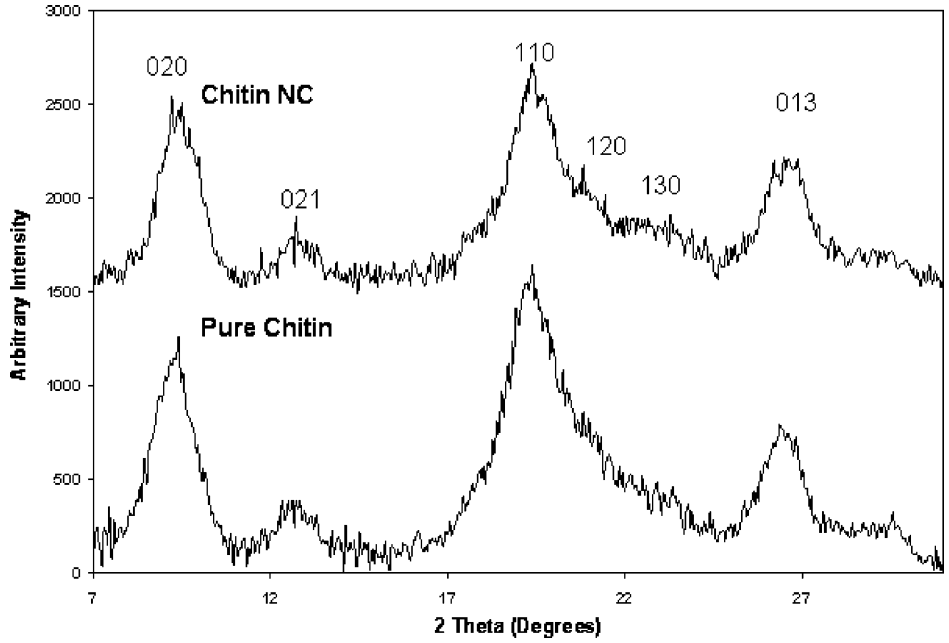

Figure 5. X-ray diffraction curves of chitin nanocrystals (top) and shrimp shell chitin before hydrolysis (bottom). *hkl* peak indexing is displayed on the top curve.

axis of the microfibrils, then the 100 and 010 sets of planes are perpendicular to the 001 planes and represent the transverse axes of the microfibrils. Line broadening from Bragg peaks representing these sets of planes or multiplicities of these planes can be used to measure crystallite widths. Crystallite dimensions for the 020 and 110 reflections were used to derive the width along the 100 set of planes, which is coincident with the crystallite width. With the high crystallinity of the particles and the apparent small transverse dimension of the particles from TEM, it can reasonably be assumed that the crystallite width corresponds well with the width of the microfibrils. Further justification for this assumption comes from a previous study on α-chitin from lobster tendons, where a strong resemblance between α-chitin microfibrils and cellulose microfibrils was observed, in that with both materials, the microfibrils were elongated single crystallites.[22] From the line broadening data, the crystallite dimensions for the chitin nanoparticles were calculated at 8.33 nm for the 100 planes and 6.65 nm for the 010 planes. This corresponds to crystallites approximately 6.65

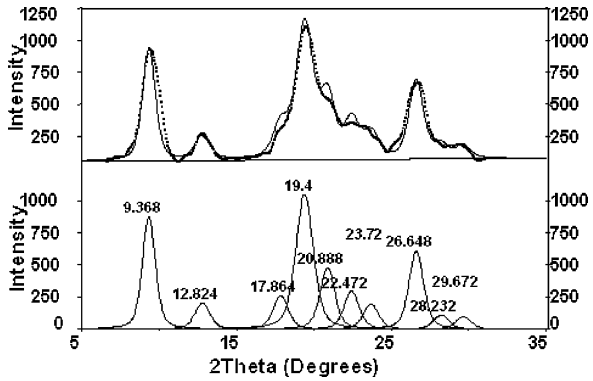

Figure 6. Deconvolution of chitin nanocrystal X-ray diffraction data. (Top) Dotted line represents smoothed data, and the solid line represents the overall fit. (Bottom) Individual peak fits. This process was repeated for the other chitin samples.

nm × 8.33 nm in cross section. If the microfibrils are assumed to have these dimensions, then the specific surface area

Table 1. Observed and Literature-Reported 2θ Values for the Six Most Intense Crystalline Diffractions Observed in the Chitin Nanocrystals[20]

hkl	$2\theta_{literature}$	$2\theta_{observed}$
020	9.39	9.37
021	12.72	12.82
110	19.30	19.40
120	20.95	20.88
130	23.54	22.47
130	26.37	26.65

approximations can be made from these dimensions without paying particular attention to particle lengths. With high aspect ratio particles such as chitin microfibrils, the specific surface area is nearly independent of the length as can be seen in Table 2 with particles of fixed transverse dimensions and variable lengths. A distribution of particle lengths is observed from the TEM micrograph in Figure 2; however, this distribution has little effect on the specific surface area.

Specific surface areas of the particles from X-ray line broadening can be approximated and compared to the surface area values from the dye binding experiments. On the basis of the transverse dimensions, an approximate particle length, and the crystal density of chitin of 1.462 g/cm^3,[20] taken as the density of the chitin nanoparticles, we calculated the surface area per gram to be approximately 370 m^2/g. The formula used to make this calculation is:

$$\mathrm{SSA} = [(4w^*l) + (2w)^2]/(\mathrm{density}^*V)$$

where w is the particle width, l is the particle length, and v is the particle volume. This value corresponds well with the specific surface area of about 350 m^2/g measured from dye binding, as will be discussed later.

Similar crystallite size measurements were performed on the unhydrolyzed chitin X-ray diffraction data, providing results that were not substantially different from those for the chitin nanocrystals. The similarity between the values indicates that the dimensions derived from the Scherrer equation correspond to domain sizes rather than particle sizes. However, with the nanocrystals approaching the size of the crystallite domains, it is not unreasonable to assume that particle dimensions are well represented by the crystallites.

Surface Area Study. The adsorption behavior of direct dyes with cellulose substrates at low dye concentrations follows Langmuir-type monolayer adsorption.[25] Congo red, as a direct dye, has been used to measure the specific surface areas of cellulosic substrates applying Langmuir adsorption theory.[13,14] We have applied similar Congo red dye adsorption techniques to both chitin and cellulose substrates, and the data indicate that the dye binding behavior can also be reasonably described by Langmuirian adsorption theory. The correlation coefficients for a linear fit of free dye concentration versus free dye concentration/dye on fiber gives values greater than 0.99 for all samples, indicating close adherence to Langmuir behavior.

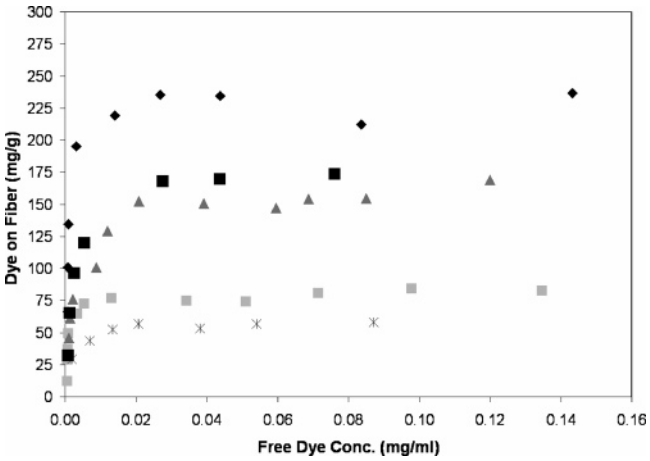

Figure 7. Langmuir isotherms of chitin and cellulose samples. Chitin nanocrystals (black ◆), chitin fibers (gray ■), pulp cellulose nanocrystals (gray ▲), bacterial cellulose nanocrystals (black ■), and pulp fibers (*).

The maximum amount of Congo red adsorbed to chitin/cellulose can be calculated by the following equation:[13]

$$[C]/[A] = 1/(K_{ads}[A]_{max}) + ([C]/[A]_{max})$$

where $[C]$ (mg/mL) is the free dye concentration at equilibrium, $[A]$ (mg dye/mg substrate) is the amount of dye adsorbed by the substrate, $[A]_{max}$ is the maximum amount of dye adsorbed onto chitin (mg/g), and K_{ads} is the adsorption equilibrium constant. Figure 7 shows the Langmuir isotherms for the chitin and cellulose substrates.

Values for $[A]_{max}$ were extracted from the reciprocal of the slope from the linear equations in a plot of free dye concentration versus free dye concentration/dye on fiber. Using the maximum amount of dye adsorbed onto the particles and the surface area of the Congo red dye molecule calculated by Inglesby and Zeronian, we calculated the specific surface area of the chitin and cellulose particles.[14] The main assumption is that the dye adsorbs parallel to the surface of the chitin or cellulose particles. Molecular modeling results produced by Woodcock et al. strongly indicate that direct dyes dock to cellulose with the longitudinal axis parallel to the polymer chains.[26] The specific surface area of a substrate can be calculated from the following relation:[13]

$$\mathrm{SSA}_{\mathrm{Substrate}} = [A]_{max} \times N_A \times \mathrm{SA}_{CR}/\mathrm{MW}$$

where N_A is Avogadro's constant, SA_{CR} is the surface area of one molecule of Congo red (1.73 nm^2), and MW is the molecular weight of Congo red (696.7 g/mol). Table 3 shows the specific surface area results for the chitin fibers and chitin and cellulose nanocrystals.

Table 2. Effect of Lateral Particle Dimensions on Specific Surface Area

transverse 1 (nm)	transverse 2 (nm)	lateral (nm)	area ($m^2 \times 10^{-15}$)	volume ($m^3 \times 10^{-24}$)	mass ($g \times 10^{-18}$)	SSA (m^2/g)
6.65	8.33	100	3.1	5.5	8.1	384
6.65	8.33	200	6.1	11.1	16.2	377
6.65	8.33	400	12.1	22.2	32.4	373
6.65	8.33	600	18.1	33.2	48.6	372
6.65	8.33	800	24.1	44.3	64.8	372
6.65	8.33	1200	36.1	66.5	97.2	371

Table 3. Dye Binding Surface Area Results

substrate	$[A]_{max}$ (mg/g)	SSA (m^2/g)
chitin fibers	83	124
chitin nanocrystals	233	347
pulp cellulose nanocrystals	167	249
bacterial cellulose nanocrystals	182	272
pulp fibers	59	88

Surprisingly, only about a 3-fold increase in specific surface area is observed for the chitin nanocrystals over the chitin fibers. From microscopic analysis, it is obvious that particle dimensions change by a few orders of magnitude, and it would be expected that surface areas would scale with the change in particle size. We think this discrepancy may be due to the presence of a high degree of internal surface area in addition to the external surface area present in the chitin fibers, which is contributing to the observation of an inordinately high total specific surface area. The internal surface area may come from voids between chitin microfibrils or microfibrillar bundles in the fibers created by protein and mineral removal. In contrast, the chitin nanocrystals are more crystalline, and the external surface is the major contributing component to the specific surface area. This same effect was observed between pulp cellulose fibers and their nanocrystals. Unfortunately, the X-ray crystallite size data could not be used for the fibers, as the crystallite dimensions describe the size of the domains rather than the size of the particles. This was not the case for the chitin nanocrystals, as the two dimensions approached the same scale. The X-ray data provide good agreement with the specific surface area measured with dye adsorption. Values from the dye adsorption experiments indicate that bacterial cellulose nanocrystals have a higher specific surface area than pulp cellulose nanocrystals, even though the transverse dimensions of bacterial cellulose microfibrils are slightly larger than those of pulp cellulose microfibrils. The discrepancy is likely because the pulp cellulose nanocrystals inevitably have residual lignin or hemicellulose materials, which are contributing to particle aggregation, thereby reducing surface area. In the absence of aggregation, based on particle sizes, pulp cellulose nanocrystals would be expected to have higher specific surface areas.

Comparing the data between chitin and cellulose nanocrystals, the specific surface area for the chitin nanocrystals is approximately 25% greater. The higher specific surface area of chitin nanocrystals over cellulose nanocrystals serves as an advantage in applications of fiber-reinforced composites. Larger surface areas allow for more contact and interaction between the fiber reinforcement and a matrix phase, in turn often enhancing the mechanical performance of the resulting material. In addition, chitin nanoparticles may offer more design versatility over cellulose, with chitin possessing both hydroxyl and amine/*N*-acetyl functionalities present on the surface for modification.

Conclusion

A dye adsorption method was used to assess the specific surface areas of chitin and cellulose nanocrystals. Results from these experiments for chitin nanocrystals were compared with microscopy and diffraction data, with a reasonable correlation existing. Further studies are in progress to prepare and characterize surface-decorated chitin nanocrystals and evaluate their performance in fiber-reinforced nanocomposites.

Acknowledgment. We gratefully acknowledge financial support from EPA-NCER Grant R830897, SUNY College of Environmental Science and Forestry, and Eastman Chemical Company.

References and Notes

(1) Muzzarelli, R. A. A. *Chitin*; Permagon: Oxford, 1977.
(2) Revol, J.-F.; Marchessault, R. H. *Int. J. Biol. Macromol.* **1993**, *15*, 329.
(3) No, H. K.; Meyers, S. P.; Lee, K. S. *J. Agric. Food Chem.* **1989**, *37*, 575.
(4) Percot, A.; Viton, C.; Domard, A. *Biomacromolecules* **2003**, *4*, 12.
(5) Li, J.; Revol, J.-F.; Marchessault, R. H. *J. Appl. Polym. Sci.* **1997**, *65*, 373.
(6) Lu, Y.; Weng, L.; Zhang, L. *Biomacromolecules* **2004**, *5*, 1046.
(7) Nair, G. K.; Dufresne, A. *Biomacromolecules* **2003**, *4*, 657.
(8) Paillet, M.; Dufresne, A. *Macromolecules* **2001**, *34*, 6527.
(9) Nair, G. K.; Dufresne, A. *Biomacromolecules* **2003**, *4*, 666.
(10) Nair, G. K.; Dufresne, A. *Biomacromolecules* **2003**, *4*, 1835.
(11) Morin, A.; Dufresne, A. *Macromolecules* **2002**, *35*, 2190.
(12) Inglesby, M. K.; Zeronian, S. H. *Cellulose* **1996**, *3*, 165.
(13) Ougiya, H.; Hioki, N.; Watanabe, K.; Morinaga, Y.; Yoshinaga, F.; Samejima, M. *Biosci. Biotechnol. Biochem.* **1998**, *62*, 1880.
(14) Inglesby, M. K.; Zeronian, S. H. *Cellulose* **2002**, *9*, 19.
(15) Raymond, L.; Morin, F. G.; Marchessault, R. H. *Carbohydr. Res.* **1993**, *246*, 331.
(16) Roman, M.; Winter, W. T. *Biomacromolecules* **2004**, *5*, 1671.
(17) Gaill, F.; Persson, J.; Sugiyama, J.; Vuong, R.; Chanzy, H. *J. Struct. Biol.* **1992**, *109*, 116.
(18) Duarte, M. L.; Ferreira, M. C.; Marvao, M. R.; Rocha, J. *Int. J. Biol. Macromol.* **2001**, *28*, 359.
(19) Tanner, S. F.; Chanzy, H.; Vincendon, M.; Roux, J. C.; Gaill, F. *Macromolecules* **1990**, *23*, 3576.
(20) Minke, R.; Blackwell, J. *J. Mol. Biol.* **1978**, *120*, 167.
(21) Hermans, P. H.; Weidinger, A. *J. Appl. Phys.* **1948**, *19*, 491.
(22) Revol, J. F. *Int. J. Biol. Macromol.* **1989**, *11*, 233.
(23) Persson, J. E.; Domard, A.; Chanzy, H. *Int. J. Biol. Macromol.* **1992**, *14*, 221.
(24) Saito, Y.; Okana, T.; Chanzy, H.; Sugiyama, J. *J. Struct. Biol.* **1995**, *114*, 218.
(25) Yoshida, H.; Kataoka, T.; Maekawa, M.; Nango, M. *Chem. Eng. J.* **1989**, *41*, B1.
(26) Woodcock, S.; Henrissat, B.; Sugiyama, J. *Biopolymers* **1995**, *36*, 201.

BM0603589